# Relationship between trapeziometacarpal joint morphological parameters and joint contact pressure: a possible factor of osteoarthritis development

Thomas Valerio, Laurent Vigouroux, Benjamin Goislard de Monsabert, Jean-Bapstiste De Villeneuve de Bargemon, Jean-Louis Milan

# Relationship between trapeziometacarpal joint morphological parameters and joint contact pressure: a possible factor of osteoarthritis development

Thomas Valerio [a,b,*], Laurent Vigouroux [a], Benjamin Goislard de Monsabert [a], Jean-Baptiste De Villeneuve Bargemon [c], Jean-Louis Milan [a,b]

[a] *Aix-Marseille University, CNRS, ISM, Marseille, France*

[b] *Aix-Marseille University, APHM, CNRS, ISM, St Marguerite Hospital, Institute for Locomotion, Department of Orthopaedics and Traumatology, Marseille, France* [c] *Department of Hand Surgery and Plastic Reconstructive Surgery of the Limbs La Timone University Hospital, Marseille, France*

ARTICLEINFO

*Keywords:*
Osteoarthritis
Trapeziometacarpal
Morphology
Finite element modelling
Contact pressures

ABSTRACT

The trapeziometacarpal (TMC) joint is the one of the hand joints that is most affected by osteoarthritis (OA). The objective of this study was to determine if specific morphological parameters could be related to the amount of pressure endured by the joint which is one of the factors contributing to the development of this pathology.

We developed 15 individualized 3D computer aided design (CAD) models of the TMC joint, each generated from the CT scan of a different participant. For each participant, we measured several crucial morphological parameters: the width and length of the trapezium bone and dorso-volar and ulno-radial curvature, of the trapezium and the metacarpal bone. Each CAD model was converted into a finite element model, of both bones and the cartilage located in between. The joint forces applied during pinch grip and power grip tasks were then applied in order to estimate the contact pressures on joint cartilage for each model. Correlations between joint contact pressures and morphology of the trapezium and the metacarpal bone were then analysed.

Important variations of TMC joint pressures were observed. For both pinch and power grip tasks, the strongest correlation with joint contact pressure was with the dorso-volar curvature of the trapezium bone.

Our findings indicate that dorso-volar curvature of the trapezium bone has a significant impact on mechanical loadings on the TMC joint. This contributes to understanding the prevalence of OA in certain patients.

## 1. Introduction

The trapeziometacarpal (TMC) joint is one of the joints most affected by osteoarthritis (OA) in the hand (Cvijeti´c et al., 2004), especially for women (Moriatis Wolf et al., 2014). This pathology is a significant health problem and lead to important functional disabilities (Miura et al., 2004). The causes of this pathology are multifactorial (Marshall et al., 2018), but the mechanical factor, i.e., the forces stresses, strain and contact pressure experienced by the joint tissues, appears to be one of the predominant factors (Anderson et al., 2011; Buckwalter et al., 2013; Droz-Bartholet et al., 2016). Nevertheless, little is known about this mechanical factor since direct measurements of the intensity of stresses/forces withstood by hand joints requires invasive methods (Rikli et al., 2007). Alternatively, those values can be indirectly estimated through biomechanical models using experimentally measured grip force, kinematics, medical imaging and electromyography as input data (Esrafilian et al., 2021). Most advanced models provide joint contact pressures for the index finger and clarify the OA risk factor associated with joint prevalence (Faudot et al., 2020).

One of the limits of those models is that the individual morphological variations are neglected by using a single joint anatomy whereas the bone morphology represents a potential factor of OA development, especially for the TMC joint (Ladd et al., 2014). Using CT scan data and statistical shape models, previous literature has shown that the TMC joint reveals high variation in morphology, in terms of trapezium length and width and first metacarpal tilt and torsion angle (Rusli and Kedgley, 2020). It has also been shown that metacarpal and trapezium bone volumes and articular surface areas in the TMC joint differ between men and women and that articular surface curvature differs according to the age and OA stage (Halilaj et al., 2014; Schneider et al., 2018; Schneider et al., 2015). These morphological variations in the TMC joint, in particular between men and women would lead to different articular contact location (Schneider et al., 2017). However, there is no quantified information on the effect of TMC bones morphology on the intensity

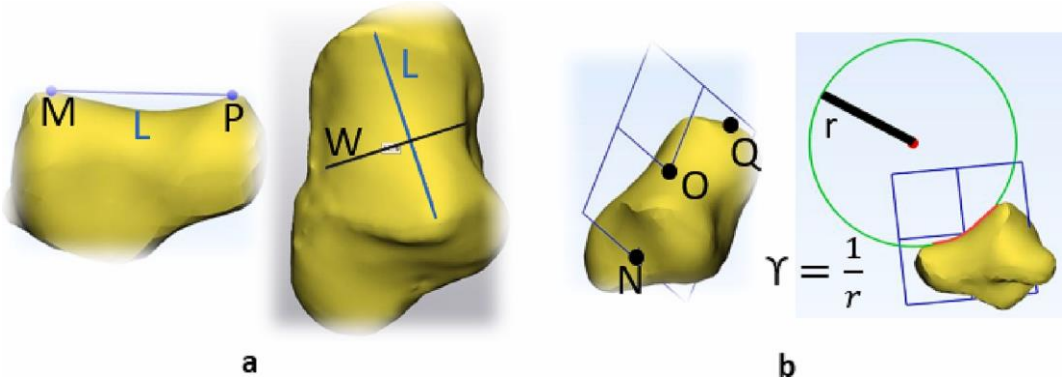


**Fig. 1.** Morphological measurement of trapezium bone length and width (a) and trapezium ulno-radial curvature ($\Upsilon_{TPUR}$) (b). Yellow bone represents the 3D CAD model of the trapezium bone for one participant. L and W (a) represent trapezium length and width measurements, respectively. Trapezium length was measured along the line between the radial (M) and ulnar (P) edges of TMC joint surface. Trapezium width was the perpendicular distance in the TMC joint surface. The blue plane and green circle (b) represent the trapezium dorso-volar mid-plane and the analytical cylinder, respectively, created to measure the curvature radius r. The mid-plane was built with three anatomical landmarks based on (Cheze et al., 2009), N,O and Q in this example. The curvature Y was assumed to be the curvature radius inverse. The same methodology was used for the other curvature measurements.

of joint mechanical loading values. Consequently, it appears crucial for the understanding of TMC OA to investigate the effect of joint morphology on joint mechanical loading values endured by cartilage tissue. This knowledge would be beneficial for prevention and rehabilitation by highlighting the specific morphological parameter that can lead to a higher risk of developing OA.

The aim of this study was to investigate the effect of morphological parameters in the TMC joint on joint contact pressures. To address this objective, patient-specific models of the TMC joint were created from CT images. We first digitally measured the size and curvature of the first metacarpal and trapezium articular surface. Then joint contact pressure was estimated using finite element analysis driven by a joint reaction force estimated from in vivo data via multi-body rigid model. We hypothesized that there is a correlation between joint contact pressure and the morphological parameters measured, especially with articular surface curvature.

## 2. Methods

### *2.1. Imaging*

CT images (slice thickness: 0.625 mm; pixel size: 0.372 mm; resolution: 512 px × 512 px) of 15 healthy patients (age: 40.9 ± 11.6 years; 9 male and 6 female; 11 right and 4 left hands) were used in this study. CT images were examined by a surgeon to ensure no OA. Among these 15 CT scans, 14 derive from the department of hand and reconstructive surgery in Marseille and were made in neutral position. The CT scan from the last participant (P7) derives from a previous study by our group (Faudot et al., 2020) and was made in pinch grip and power grip positions. This last CT scan was used as a reference to align the CT scans of the other participants in pinch grip and power grip positions with a registration method (see next part). The hand of this subject was placed in a semi-rigid cast to constrain the pinch and power grip posture. This imaging protocol was approved by the local ethics committee.

Segmentation of the first metacarpal and the trapezium bones was performed from the CT scans using Mimics (Research 22.0; Materialise, Belgium) to obtain 3D models of the TMC joint for each participant. A mirror operation was made on left hand 3D models to obtain the same coordinate system for registration.

### *2.2. Morphological measurements*

Based on the 3D TMC models, morphological measurements were done based on earlier studies which identified morphological

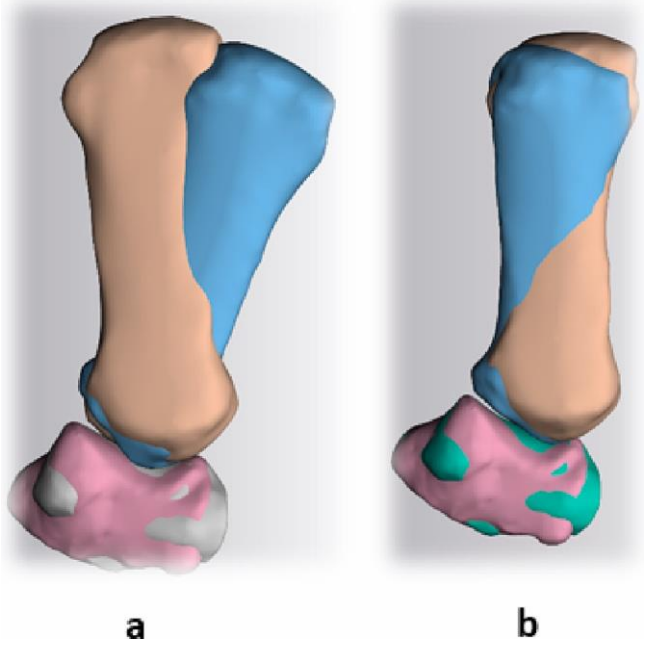


**Fig. 2.** Illustrations of the trapezium and metacarpal bone registration method used in this study for the pinch grip position of a participant. The trapezium bone of the participant in a neutral position was aligned with trapezium bone in the pinch grip position of the reference participant (a). The metacarpal bone of the participant in neutral position (blue) was then moved to be aligned with the metacarpal bone of the reference participant (beige) using rotation axis based on the previous study of (Cheze et al., 2009).

parameters with a possible important part in OA development and with an important morphological variability. These parameters were trapezium bone length and width, and dorso-volar and radio-ulnar curvature of the two bones. All these morphological measurements were performed for each participant's computer-aided design (CAD) model using 3-Matic (Research 14.0; Materialise, Belgium). Trapezium width and length measurements were made using anatomical landmarks based on previous studies (Athlani et al., 2021; Rusli and Kedgley, 2020). Briefly, the trapezium length was measured in the trapezium Kapandji plane view as the Euclidian distance between the top of the radial and ulnar TMC joint surface edges and the trapezium width as the perpendicular distance in the articular surface (Fig. 1a). Trapezium and metacarpal

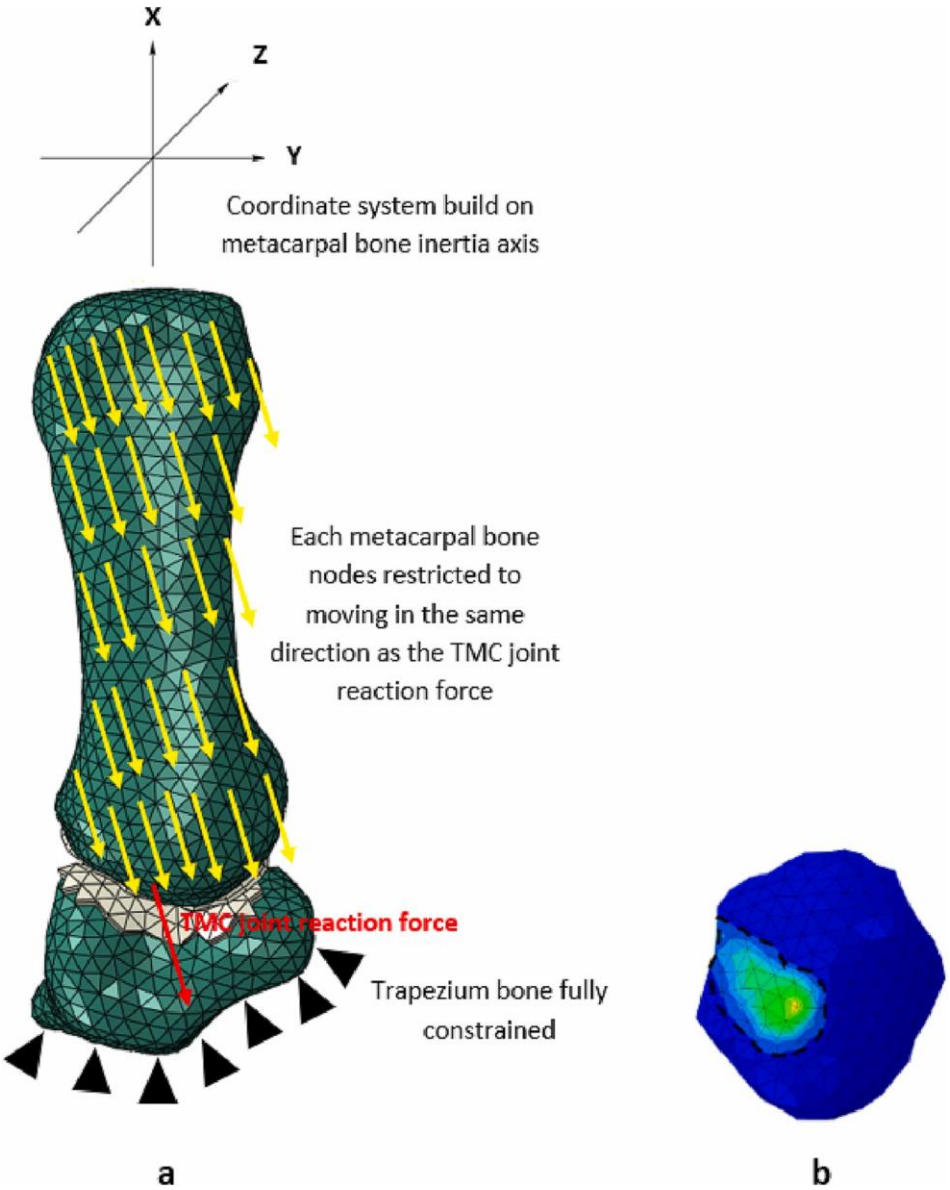


**Fig. 3.** Finite element model of one participant in the power grip position (a) and joint contact pressure distribution on cartilage surface after a simulation (b). A local coordinate system was built on the metacarpal bone inertia axis (a) and the TMC joint reaction force direction (represented in red) was determined by the multi-body rigid model of Goislard de Monsabert et al 2014 in relation to this local coordinate system. The mean TMC joint contact pressure calculated represents the average contact pressure of the articular surface area (b).

dorso-volar ($\gamma_{TPDV}$, $\gamma_{MCDV}$) and ulno-radial ($\gamma_{TPUR}$, $\gamma_{MCUR}$) curvatures were measured by fitting an analytical cylinder to the trapezium and metacarpal articular surface projected on the dorso-volar and radio- ulnar mid-plane respectively. These planes were constructed using anatomical landmarks (Cheze et al., 2009) (Fig. 1b).

### 2.3. Registration

Each trapezium bone was superposed with the reference trapezium bone in pinch grip and power grip positions (Fig. 2a). The reference participant was chosen because he performed both CT scan and motion capture analysis (for multi-body rigid model input) during the two tasks. The superposition was done using a surface-based registration method based on the iterative closest point algorithm (Besl and McKay, 1992; Cerveri et al., 2010). Thus, local coordinate systems were constructed on the trapezium and the first metacarpal bones to move the metacarpal bone in the fitting rotation axis in order to get the same pinch grip and power grip postures for each participant (Fig. 2b). These local coordinate systems were based on a previous study which determined TMC joint motion using CT scan in several different positions (Cheze et al., 2009). This operation was performed on the CAD model of each participant using 3-Matic (Research 14.0; Materialise, Belgium) to identify anatomical landmarks on each bone to construct a coordinates system. This registration method has been chosen because it minimizes the manual intervention and the error which is in the magnitude of 1° with this technique (Renault et al., 2018).

### 2.4. Finite element modelling

#### 2.4.1. Finite element model design

Finite element modelling was performed for the 15 participants in pinch grip and power grip position using Abaqus (2019; Simulia, USA). The first metacarpal and trapezium bone were meshed using quadratic tetrahedral elements (C3D10) with an edge length of 1.3 mm. Cartilage was manually created by extruding the TMC joint articular surface from the trapezium and metacarpal bones to get prismatic elements (C3D6). Cartilage thickness was assumed to be consistent across participants with an average thickness of 0.7 mm (Dourthe et al., 2019; Koff et al., 2003). Bones were modelled as linear elastic isotropic material (E = 18 GPa, $\nu$ = 0.2) and cartilage was modelled as NeoHookean hyperelastic material ($C_{10}$ = 0.34 MPa, $D_1$ = 2.20 $MPa^{-1}$) (Faudot et al., 2020). Cartilage contact in the TMC joint was modelled with a friction

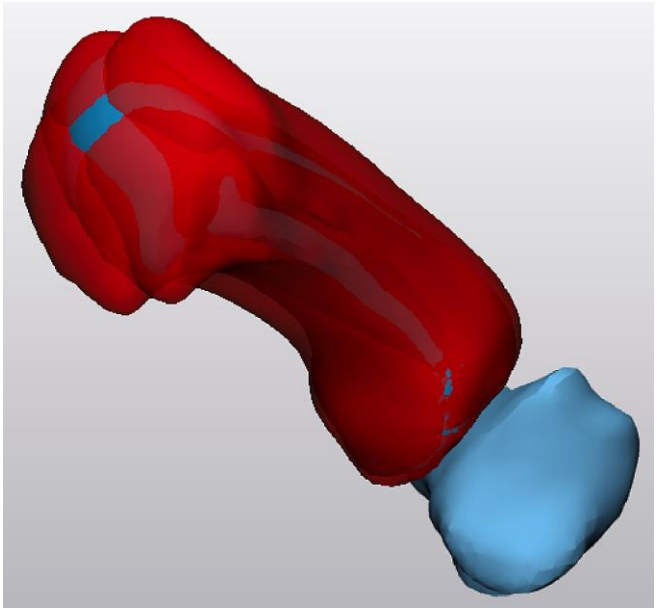

**Fig. 4.** The joint motion performed in the sensitivity analysis for one of the 15 participants. The correct joint position in our study (blue) was moved with 5° of flexion, 5° of extension, 5° of abduction and 5° of adduction (red). coefficient of 0.02 (Wright and Dowson, 1976).

*2.4.2. Loading conditions*

A TMC joint reaction force was applied on the metacarpal bone extremity to simulate the effect of force level and posture associated to the pinch grip and power grip tasks (Fig. 3a). The norm and orientation of the TMC joint force were estimated with a multi-body rigid model using finger and wrist joint angles and grip force as input. This previously developed model (Goislard de Monsabert et al., 2014) will be briefly described here as only the input data have been modified in the current study. Tendon and muscle forces were estimated by solving mechanical equilibrium equations of the hand joints. The static moments of all degrees of freedom were equilibrated using the following equation:

$[R] \times \{t\} + \{mL\} + \{mF\} = \{0\}$ (1) where [R] represents the muscle moment arms, $\{t\}$ represents the muscle tension, $\{m_L\}$ represents the passive moments due to passive tissues and $\{m_F\}$ represents the moments of external forces, i.e., the forces applied to the phalanges during grip force exertion.

To solve undetermined equation (1) (more unknown than equations), an optimization method based on the following cost function was used:

$$\left(\frac{(tm)s}{\quad}\right)^4 \quad \sum \min(2)_m \quad PCSAm$$

where $(t_m)_s$ is the muscle tension for solution $s$ and $PCSA_m$ the physiological cross-sectional area of muscle $m$.

Following the tendon force estimations, the joint reaction forces at the TMC joint were calculated using the following equation:

$$\{JR\}_j + \sum_m \{T\}_m + \sum_a \{F\}_a + \sum_l \{L\}_l = \{0\} \quad (3)$$

where $\{J_R\}_j$ is the joint reaction force for each joint $j$, $\{T\}_m$ is the tendon force for each muscle $m$, $\{F\}_a$ is the part of the applied grip force on finger area $a$ and $\{L\}_l$ is the ligament forces for each ligaments $l$.

Anatomical data were taken from An et al., 1979 for muscle moment arms and from Chao and (Ed.), 1989; Ramsay et al., 2009; Sancho-Bru et al., 2008 for PCSA. Three grip force amplitudes were simulated to consider capability differences between participants: 60, 80 and 100 N for the pinch grip task; 120, 160 and 200 N for the power grip task, based on a previous study (Goislard De Monsabert et al., 2012). To represent grip force exertion, these forces were applied at the middle of the thumb and index finger distal phalanges during the pinch grip task and shared in the entire thumb to simulate the power grip task. The pinch grip force direction and the power grip force distribution were averaged across the participants of a previous study (Goislard de Monsabert et al., 2014).

Using this methodology, the TMC joint reaction forces were calculated for each task and force amplitudes simulated to be used as an input of the finite element model.

In terms of boundary conditions for the finite element model, the trapezium bone was fully constrained, and the metacarpal bone was restricted to translate only in the same direction as the TMC joint reaction force. Joint contact pressure at each node of the TMC joint cartilage surface was calculated in each participant model for pinch grip and power grip by the Abaqus explicit solver. Then, the mean joint contact pressure was calculated by the average pressure at each node of the joint contact area (Fig. 3b) The calculation were made for all the participant bone morphology in the registration position but a sensitivity analysis of the joint position was also performed in the pinch grip position in order to ensure that the effect of morphology is not modified significantly with the joint posture. This sensitivity analysis was made by moving the metacarpal bone with 5° of flexion, 5° of extension, 5° of abduction and 5° of adduction (Fig. 4). The calculation were made also with these different joint positions.

*2.5. Statistical analysis*

Linear regression analyses with Pearson test were used to evaluate the correlation between joint contact pressure and morphological parameters. The mean joint contact pressure was considered as the response variable and the morphological parameters, namely trapezium length, trapezium width, $\Upsilon_{MCDV}$, $\Upsilon_{MCUR}$, $\Upsilon_{TPDV}$ and $\Upsilon_{TPUR}$, were considered as explanatory variables. Linear regression was done for mean joint contact pressure in pinch grip and power grip tasks to see if there is a different effect of morphology according to TMC joint position. Paired student test was also performed between the pressure increase between low and medium external force level and medium and high external force level, to see if the effect of external force on joint contact pressure is linear. The significance threshold was set at $p < 0.05$. Bonferroni corrections were applied to account for the multiple comparison in the explanatory effort.

## 3. Results

*3.1. Morphological measurements*

The mean trapezium bone length was 14.2 ± 1.7 mm (range: 10.8 – 16.1 mm) and the mean trapezium bone width was 10.2 ± 1.6 mm (range: 7.3 – 13.5 mm). The mean $\Upsilon_{MCDV}$ was 102.1 ± 22.9 $m^{-1}$ (range: 66.7 – 153.8 $m^{-1}$), the mean $\Upsilon_{MCUR}$ was 120.0 ± 15.6 $m^{-1}$ (range: 99.0 – 147.1 $m^{-1}$), the mean $\Upsilon_{TPDV}$ was 177.0 ± 43.7 $m^{-1}$ (range: 104.2 – 294.1 $m^{-1}$) and the mean $\Upsilon_{TPUR}$ was 82.1 ± 19.6 $m^{-1}$ (range: 54.9 – 117.6 $m^{-1}$).

*3.2. Joint contact pressures*

The mean joint contact pressures for each participant in pinch grip and power grip are presented in Fig. 5. Concerning the pinch grip simulation, mean joint contact pressures at the TMC joint averaged 11.7 ± 2.5 MPa (range: 6.8 – 15.8 MPa), 15.2 ± 3.2 MPa (range: 9.0 – 21.7 MPa) and 18.8 ± 4.1 MPa (range: 11.2 – 26.1 MPa) for the 60, 80 and 100 N external force levels respectively. Concerning the power grip simulation, the TMC joint pressure average values were 8.5 ± 1.5 MPa (range: 6.2 – 11.7 MPa), 10.4 ± 1.8 MPa (range: 7.6 – 14.1 MPa) and 12.4 ± 2.2 MPa (range: 9.2 – 17.0 MPa) for the 120, 160 and 200 N

**Fig. 5.** Joint contact pressure at the TMC joint for the 15 participants, during the two tasks. These values were calculated by averaging the contact pressure at each node of the cartilage surface contact area. The values obtained with the low, medium and high external forces are presented in blue, orange and gray respectively for the two tasks.

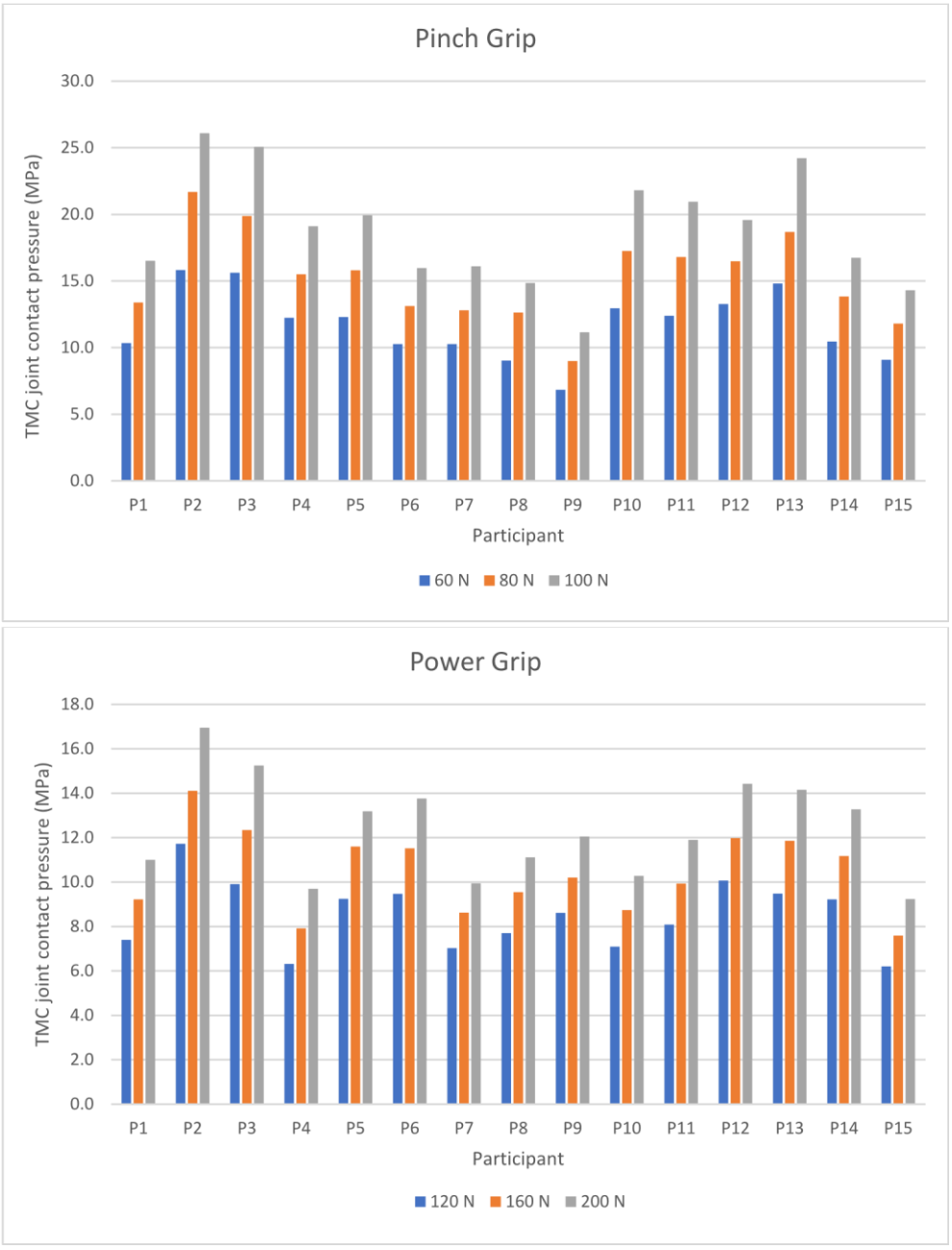


external force levels respectively.

### 3.3. *Relationship between joint contact pressure and morphology*

The joint contact pressure results reveal a linear relation between an increase in pinch and power grip external forces and TMC joint contact pressure (Fig. 5). Paired student test reveals that pressure increase is the same from 60 to 80 N and from 80 to 100 N in the pinch grip position ($p = 0.82$). The same effect is observed in power grip position ($p = 0.32$). For this reason, only the results of the linear regression for the simulations with 60 N in pinch grip and 120 N in power grip are presented. The linear regression results are summarized in Table 1. In the pinch grip position, the best fitting linear model (with the highest $r^2$ and the lowest p value) was the model with $Y_{TPDV}$ as an explanatory variable. A significant correlation was observed between this variable and the mean TMC joint contact pressures of the participants ($r^2 = 0.62$; $p < 0.002$). A significant correlation was also found between pinch grip joint pressure and the trapezium length ($r^2 = 0.58$; $p < 0.002$). In the power grip position, the best-fitting linear model was the one with $Y_{TPDV}$ as an explanatory variable ($r^2 = 0.51$; $p < 0.008$). Plots of the two best linear regression models in pinch grip and power grip positions are presented in Fig. 6.

## 4. Discussion

The objectives of this study were to investigate the effect of morphological variation of the TMC joint on joint contact pressure. To answer this objective, trapezium length and width and TMC joint

**Table 1**
Multiple $r^2$ and p value of each linear regression model between TMC joint contact pressures and morphological variables.

| Variables | R- squared | P value |
|---|---|---|
| Pinch Grip **ϒ** | | |
| **TPDV** | **0.62** | **0.0005**** |
| ϒ TPUR | 0.002 | 0.9 |
| ϒ MCDV | 0.003 | 0.9 |
| ϒ MCUR | 0.16 | 0.1 |
| Trapezium Width | 0.40 | 0.01 |
| Trapezium Length | 0.58 | 0.0009** |
| Power Grip **ϒ** | | |
| **TPDV** | **0.51** | **0.003*** |
| ϒ TPUR | 0.01 | 0.7 |
| ϒ MCDV | 0.04 | 0.5 |
| ϒ MCUR | 0.24 | 0.07 |
| Trapezium Width | 0.26 | 0.05 |
| Trapezium Length | 0.20 | 0.1 |

*Note.* Bold models represent the best linear regression model

principal curvatures were measured on 15 TMC joints of healthy participants. Then, finite element models were developed for each participant to simulate pinch grip and power grip tasks. The finite element model was driven by a joint reaction force estimated using in vivo motion capture, via a previously developed multi-body rigid modelling. Finally, correlations between these morphological variations and TMC joint contact pressure were analysed by linear regression.

Morphological measurements of trapezium length, trapezium width, $\gamma_{TPDV}$, $\gamma_{TPUR}$ and $\gamma_{MCUR}$ were consistent with more population samples (Athlani et al., 2021; Halilaj et al., 2014; Marzke et al., 2012, 2009; Rusli and Kedgley, 2020; Shih et al., 2018). Some differences were found for $\gamma_{MCDV}$ with 82 % difference from the mean values of Halilaj et al., 2014. This difference could be explained by this morphological measure might be less accurate or repeatable because the articular surfaces are manually selected from the subchondral bone. Previous literature has also observed discrepancies in the $\gamma_{MCDV}$ value between studies (Halilaj et al., 2014; Shih et al., 2018). Except for this parameter, the similar ranges between this current study and previous literature suggest that the sample used was representative of the population, in terms of TMC joint morphology. This verification was essential to study the effect of morphological variation on joint contact pressure, given the small size of the sample in the current study.

Joint contact pressure values were consistent with previous literature on the same simulated task and force amplitudes (Goislard de Monsabert et al., 2014). In comparison to this previous study, mean contact pressure values observed here differ by 26 % in the pinch grip position and by 27 % in the power grip position, for 60 and 120 N force levels respectively. These differences could be due to the pressure estimation methods. In Goislard de Monsabert et al., 2014, the mean joint pressure was calculated by dividing the TMC joint reaction force by a joint contact area estimation, while in the current study they are computed using a finite element model. The non-inclusion of tissues' mechanical properties in the study of Goislard de Monsabert et al., 2014) may reduce the accuracy of joint contact pressure estimation in comparison with the finite element method.

For 14 participants, joint contact pressure in the pinch grip position was larger than in the power grip position, which is consistent with previous literature (Goislard de Monsabert et al., 2014). In only one participant (P9), joint contact pressure was larger in the power grip position. This participant presented a lower joint contact pressure level and a lower $\gamma_{TPDV}$. Given that dorso-volar curvature has the best correlation with joint contact pressure compared to the other morphological parameters (Table. 1), it can be hypothesized that this morphological abnormality explains the individual different effects of position. The current result suggests that there may be an interaction between joint position and morphology, given that force and kinematic input data were the same for each participant.

The linear regression analysis results (Table 1) indicate that the variation of joint contact pressure across participants could be related to dorso-volar curvature of the trapezium ($\gamma_{TPDV}$) in both pinch grip and power grip positions. This confirms our hypothesis on the joint curvature effect on contact pressure. This significant correlation could be explained by the location of the peak contact pressure which is located almost always at the trapezium central-ulnar side for all the participants. At this location the $\gamma_{TPDV}$ gradient seems to be larger than the other curvatures and we can suppose that this curvature lead to the principal effect on the joint contact pressures in this manner. Therefore, the regression results showed that the more $\gamma_{TPDV}$ is large, the larger joint

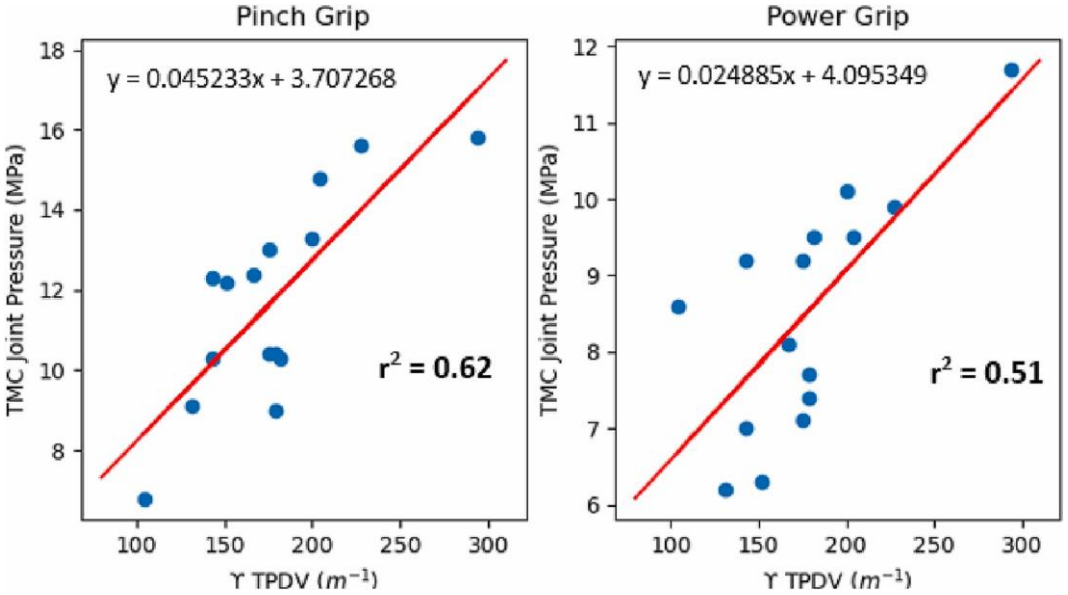


**Fig. 6.** Best-fitting linear regression models for pinch and power grip position simulations with 60 and 120 N, respectively. Mean joint contact pressure at the TMC joint for each participant is represented by blue points. The red line represents the regression line. This figure represents the relationship between the best morphological explanatory variable and the mean joint contact pressures at the TMC joint. The best morphological explanatory variable is the trapezium dorso-volar curvature $\gamma_{TPDV}$ for the two positions.

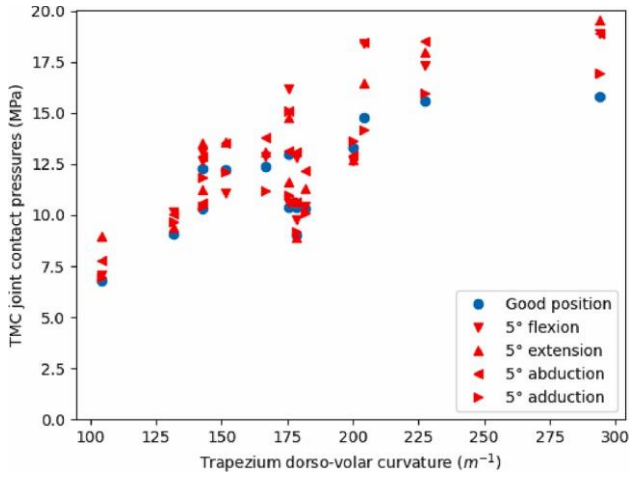


**Fig. 7.** Results of the sensitivity analysis for all the participants. The blue points represent the relationship between joint contact pressure and trapezium dorso- volar curvature in the good pinch grip position. The red triangles represent this relationship in the four moved pinch grip positions.

contact pressures are. This point is crucial since it corroborates previous literature which has shown that early TMC OA is also associated with a large $\Upsilon_{TPDV}$ (Halilaj et al., 2014). The current study highlights the fact that a high $\Upsilon_{TPDV}$ could be a risk factor for TMC OA. The significant correlation with trapezium length, during the pinch grip position could indicate another potential TMC OA risk factor and corroborates previous literature suggesting a link between this morphological parameter and the potential development of TMC OA (Ladd et al., 2015). Nevertheless, the correlation was only significant with pinch grip, meaning that certain morphology could be at risk when associated to specific tasks. The weak correlation with the other morphological measurements seems to indicate that these morphological parameters do not play a crucial role in the modulation of pressures and thus on the development of TMC OA. Nevertheless, other tasks should be tested to confirm this idea as our results only focused on pinch grip and power grip tasks whereas, as mentioned above, some morphological parameters might be correlated to joint mechanical loading in specific tasks.

This study shows a significant effect of the variations of TMC joint morphology on joint contact pressures, especially with $\Upsilon_{TPDV}$. Considering mechanical loading is an important OA risk factor (Buckwalter et al., 2013; Droz-Bartholet et al., 2016), this morphological parameter could have a key role in OA development. Consequently, our results might be applied to detect an OA risk in patients based on simple measurement from medical imaging. Detected patients could then be advised to either reduce the load they carry or adapt their daily life to avoid certain grip techniques.

Some limitations should be considered. First, we only simulated two tasks while daily life activities require more complex loading, for example jar twist, which can influence joint contact pressure differently (Schneider et al., 2017). Another limitation is the TMC joint position in pinch grip and power grip tasks which were standardized in the same position as the reference participant. Joint posture indeed can differs across participants for a same task, which further influence muscle forces and ultimately joint contact pressure (Faudot et al., 2020; Goislard de Monsabert et al., 2014). However, the sensitivity analysis (Fig. 7) of the TMC joint position on contact pressure has shown that the morphology effect seems to be more important than position effect. The multi-body rigid and finite element models used in this study include some other limitations like modeling hypothesis and lack of direct validation, even if this method is the only way to estimate joint contact pressure. Curvature measurements in a plane could be another limitation considering that it varies spatially. The different ligamentous constrains between participants were not modelled, but ligament of TMC joint seems slack in the modelled position and their contributions are probably negligible (Halilaj et al., 2015). The number of participants could also be another limitation of this study as morphological variations can be large in the population. Nevertheless, the morphological parameter ranges in the current sample are consistent with the values from previous studies that included larger samples.

Despite these limitations, this study provides interesting new information that may contribute to our understanding of the development of TMC OA. The current study reveals that trapezium dorso-volar curvature is correlated with higher joint contact pressure. Based on our study outcomes, further studies on TMC OA development should focus on possible correlation with this curvature, including patient specific orientation and an extremely large number of patients.

## CRediT authorship contribution statement

**Thomas Valerio:** Validation, Software, Resources, Project administration, Methodology, Investigation, Funding acquisition, Formal analysis, Data curation, Conceptualization. **Laurent Vigouroux:** Supervision. **Benjamin Goislard de Monsabert:** Supervision. **Jean- Baptiste De Villeneuve Bargemon:** Supervision. **Jean-Louis Milan:** Supervision.

## Declaration of Competing Interest

The authors declare that they have no known competing financial interests or personal relationships that could have appeared to influence the work reported in this paper.

## References

An, K.N., Chao, E.Y., Cooney, W.P., Linscheid, R.L., 1979. Normative model of human hand for biomechanical analysis. J. Biomech. 12, 775–788. https://doi.org/ 10.1016/0021-9290(79)90163-5.

Anderson, D.D., Van Hofwegen, C., Marsh, J.L., Brown, T.D., 2011. Is elevated contact stress predictive of post-traumatic osteoarthritis for imprecisely reduced tibial plafond fractures?: contact stress predicts post-traumatic OA. J. Orthop. Res. 29, 33–39. https://doi.org/10.1002/jor.21202.

Athlani, L., Auberson, L., Motte, D., Moissenet, F., Beaulieu, J.-Y., 2021. Comparison of two radiographic landmarks for centering the trapezial component in total trapeziometacarpal arthroplasty. Hand Surg. Rehabil. 40, 609–613. https://doi.org/ 10.1016/j.hansur.2021.05.002.

Besl, P.J., McKay, N.D., 1992. A method for registration of 3-D shapes. IEEE Trans. Pattern Anal. Mach. Intell. 14, 239–256. https://doi.org/10.1109/34.121791.

Buckwalter, J.A., Anderson, D.D., Brown, T.D., Tochigi, Y., Martin, J.A., 2013. The Roles of Mechanical Stresses in the Pathogenesis of Osteoarthritis: Implications for Treatment of Joint Injuries. Cartilage 4, 286–294. https://doi.org/10.1177/ 1947603513495889.

Cerveri, P., De Momi, E., Marchente, M., Baud-Bovy, G., Scifo, P., Barros, R.M.L., Ferrigno, G., 2010. Method for the estimation of a double hinge kinematic model for the trapeziometacarpal joint using MR imaging. Comput. Methods Biomech. Biomed. Engin. 13, 387–396. https://doi.org/10.1080/10255840903260818.

Chao, E.Y. (Ed.), 1989. Biomechanics of the hand: a basic research study. World Scientific, Singapore ; Teaneck, N.J.

Cheze, L., Dumas, R., Comtet, J.J., Rumelhart, C., Fayet, M., 2009. A joint coordinate system proposal for the study of the trapeziometacarpal joint kinematics. Comput. Methods Biomech. Biomed. Engin. 12, 277–282. https://doi.org/10.1080/ 10255840802459404.

Cvijeti´c, S., Kurtagi´c, N., Ozegovi´c, D.D., 2004. Osteoarthritis of the hands in the rural population: a follow-up study. Eur. J. Epidemiol. 19, 687–691. https://doi.org/ 10.1023/b:ejep.0000036794.40723.8e.

Dourthe, B., Nickmanesh, R., Wilson, D.R., D'Agostino, P., Patwa, A.N., Grinstaff, M.W., Snyder, B.D., Vereecke, E., 2019. Assessment of healthy trapeziometacarpal cartilage properties using indentation testing and contrast-enhanced computed tomography. Clin. Biomech. 61, 181–189. https://doi.org/10.1016/j.clinbiomech.2018.12.015.

Droz-Bartholet, F., Verhoeven, F., Prati, C., Wendling, D., 2016. Prevention of Hand Osteoarthritis by Hemiparesis. Arthritis Rheumatol. 68, 647–647. https://doi.org/ 10.1002/art.39512.

Esrafilian, A., Stenroth, L., Mononen, M.E., Vartiainen, P., Tanska, P., Karjalainen, P.A., Suomalainen, J.S., Arokoski, J., Lloyd, D.G., Korhonen, R.K., 2021. An EMG-assisted Muscle-Force Driven Finite Element Analysis Pipeline to Investigate Joint- and Tissue-Level Mechanical Responses in Functional Activities: Towards a Rapid Assessment Toolbox (preprint). Biophysics. https://doi.org/10.1101/ 2021.03.27.436509.

Faudot, B., Milan, J.-L., Goislard de Monsabert, B., Le Corroller, T., Vigouroux, L., 2020. Estimation of joint contact pressure in the index finger using a hybrid finite element musculoskeletal approach. Comput. Methods Biomech. Biomed. Engin. 23, 1225–1235. https://doi.org/10.1080/10255842.2020.1793965.

Goislard De Monsabert, B., Rossi, J., Berton, E., Vigouroux, L., 2012. Quantification of Hand and Forearm Muscle Forces during a Maximal Power Grip Task. Med. Sci. Sports Exerc. 44, 1906–1916. https://doi.org/10.1249/MSS.0b013e31825d9612.

Goislard de Monsabert, B., Vigouroux, L., Bendahan, D., Berton, E., 2014. Quantification of finger joint loadings using musculoskeletal modelling clarifies mechanical risk factors of hand osteoarthritis. Med. Eng. Phys. 36, 177–184. https://doi.org/10.1016/j.medengphy.2013.10.007.

Halilaj, E., Moore, D.C., Laidlaw, D.H., Got, C.J., Weiss, A.-P.-C., Ladd, A.L., Crisco, J.J., 2014. The morphology of the thumb carpometacarpal joint does not differ between men and women, but changes with aging and early osteoarthritis. J. Biomech. 47, 2709–2714. https://doi.org/10.1016/j.jbiomech.2014.05.005.

Halilaj, E., Rainbow, M.J., Moore, D.C., Laidlaw, D.H., Weiss, A.-P.-C., Ladd, A.L., Crisco, J.J., 2015. In vivo recruitment patterns in the anterior oblique and dorsoradial ligaments of the first carpometacarpal joint. J. Biomech. 48, 1893–1898. https://doi.org/10.1016/j.jbiomech.2015.04.028.

Koff, M.F., Ugwonali, O.F., Strauch, R.J., Rosenwasser, M.P., Ateshian, G.A., Mow, V.C., 2003. Sequential wear patterns of the articular cartilage of the thumb carpometacarpal joint in osteoarthritis. J. Hand Surg. 28, 597–604. https://doi.org/ 10.1016/S0363-5023(03)00145-X.

Ladd, A.L., Crisco, J.J., Hagert, E., Rose, J., Weiss, A.-P.-C., 2014. The 2014 ABJS Nicolas Andry Award: The puzzle of the thumb: mobility, stability, and demands in opposition. Clin. Orthop. 472, 3605–3622. https://doi.org/10.1007/s11999-014- 3901-6.

Ladd, A.L., Messana, J.M., Berger, A.J., Weiss, A.-P.-C., 2015. Correlation of clinical disease severity to radiographic thumb osteoarthritis index. J. Hand Surg. 40, 474–482. https://doi.org/10.1016/j.jhsa.2014.11.021.

Marshall, M., Watt, F.E., Vincent, T.L., Dziedzic, K., 2018. Hand osteoarthritis: clinical phenotypes, molecular mechanisms and disease management. Nat. Rev. Rheumatol. 14, 641–656. https://doi.org/10.1038/s41584-018-0095-4.

Marzke, M.W., Tocheri, M.W., Steinberg, B., Femiani, J.D., Reece, S.P., Linscheid, R.L., Orr, C.M., Marzke, R.F., 2009. Comparative 3D quantitative analyses of trapeziometacarpal joint surface curvatures among living catarrhines and fossil hominins. Am. J. Phys. Anthropol. NA-NA. https://doi.org/10.1002/ajpa.21112.

Marzke, M.W., Tocheri, M.W., Marzke, R.F., Femiani, J.D., 2012. Three-Dimensional Quantitative Comparative Analysis of Trapezial-Metacarpal Joint Surface Curvatures in Human Populations. J. Hand Surg. 37, 72–76. https://doi.org/10.1016/j. jhsa.2011.09.007.

Miura, T., Ohe, T., Masuko, T., 2004. Comparative in vivo kinematic analysis of normal and osteoarthritic trapeziometacarpal joints. J. Hand Surg. 29, 252–257. https://doi.org/10.1016/j.jhsa.2003.11.002.

Moriatis Wolf, J., Turkiewicz, A., Atroshi, I., Englund, M., 2014. Prevalence of doctor- diagnosed thumb carpometacarpal joint osteoarthritis: an analysis of Swedish health care. Arthritis Care Res. 66, 961–965. https://doi.org/10.1002/acr.22250.

Ramsay, J.W., Hunter, B.V., Gonzalez, R.V., 2009. Muscle moment arm and normalized moment contributions as reference data for musculoskeletal elbow and wrist joint models. J. Biomech. 42, 463–473. https://doi.org/10.1016/j.jbiomech.2008.11.035.

Renault, J.-B., Aüllo-Rasser, G., Donnez, M., Parratte, S., Chabrand, P., 2018. Articular- surface-based automatic anatomical coordinate systems for the knee bones. J. Biomech. 80, 171–178. https://doi.org/10.1016/j.jbiomech.2018.08.028.

Rikli, D.A., Honigmann, P., Babst, R., Cristalli, A., Morlock, M.M., Mittlmeier, T., 2007. Intra-articular pressure measurement in the radioulnocarpal joint using a novel sensor: in vitro and in vivo results. J. Hand Surg. 32, 67–75. https://doi.org/ 10.1016/j.jhsa.2006.10.007.

Rusli, W.M.R., Kedgley, A.E., 2020. Statistical shape modelling of the first carpometacarpal joint reveals high variation in morphology. Biomech. Model. Mechanobiol. 19, 1203–1210. https://doi.org/10.1007/s10237-019-01257-8.

Sancho-Bru, J.L., Vergara, M., Rodríguez-Cervantes, P.-J., Giurintano, D.J., P´erez-Gonzalez, A., 2008. Scalability of the Muscular Action in a Parametric 3D Model of ´ the Index Finger. Ann. Biomed. Eng. 36, 102–107. https://doi.org/10.1007/s10439- 007-9395-6.

Schneider, M.T.Y., Zhang, J., Crisco, J.J., Weiss, A.P.C., Ladd, A.L., Nielsen, P., Besier, T., 2015. Men and women have similarly shaped carpometacarpal joint bones. J. Biomech. 48, 3420–3426. https://doi.org/10.1016/j.jbiomech.2015.05.031.

Schneider, M.T.Y., Zhang, J., Crisco, J.J., Weiss, A.-P.-C., Ladd, A.L., Mithraratne, K., Nielsen, P., Besier, T., 2017. Trapeziometacarpal joint contact varies between men and women during three isometric functional tasks. Med. Eng. Phys. 50, 43–49. https://doi.org/10.1016/j.medengphy.2017.09.002.

Schneider, M.T.Y., Zhang, J., Walker, C.G., Crisco, J.J., Weiss, A.-P.-C., Ladd, A.L., Nielsen, P.M.F., Besier, T., 2018. Early morphologic changes in trapeziometacarpal joint bones with osteoarthritis. Osteoarthritis Cartilage 26, 1338–1344. https://doi.org/10.1016/j.joca.2018.06.008.

Shih, J.G., Mainprize, J.G., Binhammer, P.A., 2018. Comparison of computed tomography articular surface geometry of male versus female thumb carpometacarpal joints. Hand 13, 33–39. https://doi.org/10.1177/ 1558944716688528.

Wright, V., Dowson, D., 1976. Lubrication and cartilage. J. Anat. 121, 107–118.